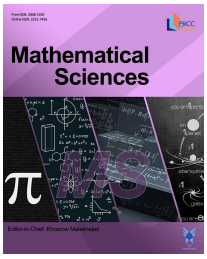

Math. Sci. 2025; 19(2) : 1-16

Mathematical Sciences (MS)

https://doi.org/10.57647/mathsci.2025.1902.09

Chebyshev wavelets for solving two-dimensional multi-noise stochastic integral equations in combination with block pulse functions

Azadeh Biabani, Morteza Khodabin*, Reza Ezzati, Mohsen Fallahpour

Department of Mathematics, Ka. C., Islamic Azad University, Karaj, Iran

***Corresponding author:** m-khodabin@iau.ac.ir

Original Research

Received:
25 April 2025

Revised:
02 June 2025

Accepted:
13 June 2025

Published online:
30 June 2025

Abstract:

In this investigation, our goal is to numerically solve two-dimensional Volterra-Fredholm stochastic integral equations with multiple perturbations, using two-dimensional Chebyshev wavelets of the second kind as unitary orthogonal bases. For this purpose, after rewriting the functions in the stochastic integral equation based on two-dimensional Chebyshev wavelets of the second kind, to construct ordinary and random operational matrices, we expand these wavelets based on block pulse functions and, with the help of these expansions, obtain the desired operational matrices. These matrices result in a linear system, the solution of which will lead to the numerical solution of our stochastic integral equation. The estimation and analysis of the convergence of the proposed method, along with the examples provided, the average error at different points, the %95 confidence interval and the comparison of our method with other common methods, demonstrate the efficiency and accuracy of this method well.

Keywords: Numerical method; Chebyshev wavelets; Block-pulse functions; Two-dimensional stochastic integral; Volterra-Fredholm integral

Cite this article: Biabani A., Khodabin M., Ezzati R., Fallahpour M., Chebyshev wavelets for solving two-dimensional multi-noise stochastic integral equations in combination with block pulse functions. Math. Sci 2025; *19*(2) : 1-16 https://doi.org/10.57647/mathsci.2025.1902.09

1. Introduction

At the beginning of this section, in order to familiarize readers interested in researching the solution of stochastic integral equations, we will first briefly discuss how a stochastic integral equation is formed. As all researchers in this field of science know well, when a white noise $\xi(x)$ enters an ordinary differential equation such as

$$\frac{dg(x)}{dx} = ag(x),$$

it transforms that equation into a one-dimensional stochastic differential equation. If this white noise enters the said equation collectively, we have [1]

$$\frac{dg(x)}{dx} = ag(x) + \xi(x), \rightarrow dg(x) = ag(x)dx + dB(x).$$

This corresponds to a one-dimensional stochastic integral equation of the form

$$g(x) = g(x_0) + \int_{x_0}^{x} ag(s)ds + \int_{x_0}^{x} dB(s).$$

Also, if the aforementioned white noise is entered into the desired ordinary differential equation in a multiplicative manner, we have

$$\frac{dg(x)}{dx} = (a + \xi(x))g(x), \rightarrow dg(x) = ag(x)dx + g(x)dB(x),$$

where the form of a one-dimensional stochastic integral equation like this will be as

$$g(x) = g(x_0) + \int_{x_0}^{x} ag(s)ds + \int_{x_0}^{x} g(s)dB(s).$$

Similarly, two-dimensional stochastic integral equations arise after a two-dimensional noise $\xi(x, y)$ is introduced additively or multiplicatively into a partial differential

equation. In the following, we will examine one type of such equations. The background of research in solving stochastic integral equations leads every researcher towards studies in various fields of science, such as finance, engineering, physics, chemistry, mechanics, biology, medical,social sciences, ecology, technology, etc [2, 3, 1, 4]. Investigations in these areas have so far resulted in the numerical solution of stochastic integral equations in one and two dimensions, some of which are given in references [5, 6, 7, 8, 9, 10, 11, 12, 13, 14] Most of these stochastic equations do not have an analytical solution or obtaining an analytical solution for them has its own difficulties. This difficulty in obtaining the solution of a two-dimensional $(2D)$ stochastic integral equation is doubly high because the random functions appearing in $2D$ stochastic equations are bivariate and quadratic, and naturally the volume of stochastic calculations in such equations is very high. Now consider that an integral equation, in addition to being stochastic and $2D$, also has multiple noises. Our goal in this article is to solve the $2D$ multiple noises stochastic Volterra-Fredholm linear integral equations $(2D.MN.S.VF.LIEs)$, and to achieve this goal, we are forced to use the numerical methods. Here there is a fundamental difference in the numerical solutions of an ordinary integral equation and a stochastic integral equation, that is in the first case, what is important for the researcher is that the difference between the numerical solutions and the analytical solution of the equation (the error of the method), is very small, but in the second case, in addition to the fact that our mind is busy with the error of the presented method, we must check the %95 confidence interval $(\overbrace{\%95CI})$ and the error mean in every point regularly. That is, in solving stochastic equations, after repeating our method several times to solve the desired stochastic equation, we should expect that the solutions one after the other will fall within a specific and reliable interval with a probability of %95. In fact, it can be admitted that as the length of the %95 confidence interval $(\overline{L\%95CI})$ decreases, as the error mean at the target point will also become less and less, that it means the approximate solutions become closer to each other and in the same way these approximate solutions converge to the analytical solution of the equation. As can be seen from the research related to the field of solving integral equations, many attempts have been made to solve these equations, both ordinary and stochastic, in one and two dimensions. One of the interesting ideas for solving such equations is the composition plan of the basis functions together that in this regard, ordinary and stochastic integral equations have been solved well numerically [5, 6, 8, 14, 15]. Therefore, we and other researchers are always trying to provide new combined methods for numerically solving $2D$ stochastic integral equations and in future research, we will compare and evaluate these methods with previous methods. One of these combined methods can be the combination of Chebyshev wavelets with block pulse functions. Due to the simplicity of working with block pulse functions and the special properties of these functions such as disjointness, orthogonality and completeness, we can combine any of the basic functions with them and thus achieve a new combined numerical method. Although the direct use of Chebyshev wavelets based on the collocation techniques of similar polynomials is itself a numerical method for solving $2D$ stochastic integral equations, when we encounter problems such as the existence of non-smooth stochastic kernels, local adaptivity and tensor product complexities, then combining the Chebyshev wavelet method with simple block pulse functions paves the way for numerical solution for us. In fact, it can be admitted that when we are faced with the aforementioned problems, then the volume of our computational operations in dealing with polynomial, exponential and Chebyshev operational matrices will be difficult, long and time-consuming. While when we combine Chebyshev wavelets with block pulse functions, we witness the emergence of simpler operational matrices with less computational volume, and this is the strength and novelty of using such combined methods. This is a surprise when the $2D$ stochastic integral equation of interest has multiple noises, in two different dimensions. It is worth mentioning here the recent efforts made by researchers in the field of using various Chebyshev wavelets to solve ordinary differential equations [16, 17, 18, 19, 20, 21, 22] and it is also suggested that Chebyshev polynomials be used in the study of generalized fractional models, which could be part of new research by researchers in this field [23, 24, 25]. In this research, our intention is to use a combination of Chebyshev wavelets with block pulse functions to solve the $2D.MN.S.VF.LIE$

$$g(x,y) = f(x,y) + \int_0^1 \int_0^1 u_1(x,y,s,t)g(s,t)dsdt + \int_0^y \int_0^x u_2(x,y,s,t)g(s,t)dsdt + \sum_{i=1}^{\iota_1} \sum_{j=1}^{\iota_2} \int_0^y \int_0^x u_3(x,y,s,t)g(s,t)dB_i(s)dB_j(t), \quad (1)$$

for $(s,t) \in [0,1]^2$ and $(x,y,s,t) \in [0,1]^4$, where $f(x,y)$ and u_t, $t = 1,2,3$ are the known stochastic processes defined on probability space $(\mathbf{\Omega}, \mathcal{F}, \mathbb{P})$, while $g(x,y)$ is an unknown function and is called the function of the solution of Eq. (1). By the way, each of the sets $B_1(s), B_2(s), ...B_{\iota_1}(s)$ and $B_1(t), B_2(t), ...B_{\iota_2}(t)$ are ι_1 and ι_2 independent Brownian motions on $\mathbb{R}$, respectively. But what we want to do to solve Eq. (1), is that in the first step, we expand all the functions in this equation based on $2D$ Chebyshev wavelets of the second kind $(2D - CWs^{2k})$. Then, in order to construct the ordinary Fredholm operational matrix and also construct the ordinary and stochastic Volterra operational matrices, this time we expand the $2D - CWs^{2k}$ based on $2D$ block pulse functions $2D - BPFs$, then using the relations between the two basic Chebyshev and block pulse functions, we obtain the operational matrices of our equation based on the $2D - CWs^{2k}$. Therefore we

https://doi.org/10.57647/mathsci.2025.1902.09

arrive at a linear system of equations and perform the numerical solution of the obtained system and arrive at the answer matrix.

The configuration of this article is based on the following strategy:

In Section 2, after introducing some crucial concepts about $2D-BPFs$, eigen orthogonal Chebyshev polynomials, and then $2D-CWs^{2k}$, we will examine the relationship between $2D-CWs^{2k}$ and $2D-BPFs$. Then, in Section 3, after a review of the operational matrices of $2D-BPFs$, we will calculate the operational matrices of $2D-CWs^{2k}$. In the next section, we will use the $2D-CWs^{2k}$ method combined with $2D-BPFs$ to solve our original equation. In Section 5, we will analyze and decompose how the approximate solutions obtained from the proposed method converge to the analytical solution of our equation by presenting some basic theorems. Also in this section, we present the algorithm of the desired method for implementing the original equation solving program. In section 6, to show the efficiency and accuracy of the current method, while presenting some examples, we have compared our method with some other numerical methods and in this section, %95CIs have been obtained for each answer obtained at each desired point. Finally, the conclusion part is given in section 7.

2. Required terminology for functions used

In this section, we first explain important and basic points about block pulse, first and second types of Chebyshev polynomials, first and second types of Chebyshev wavelets, and finally the relationship between Chebyshev wavelets and block pulses, along with the concepts required for these functions to be used in the main method of this article.

2.1 Block pulse functions

Recalling the basic concepts of $2D-BPFs$ an (n_1n_2)-set of $2D-BPFs$ $\breve{b_p}^{i,j}(x,y)$, $i=1,2,\ldots,n_1$, $j=1,2,\ldots,n_2$; are defined in $(x,y)\in[0,T_1)\times[0,T_2)$ as

$$\breve{b_p}^{i,j}(x,y)=\begin{cases}1, & for\begin{cases}(i-1)v_1\le x<iv_1\\(j-1)v_2\le y<jv_2\end{cases}\\0, & otherwise\end{cases},$$

where

$$v_t=\frac{T_t}{n_t},\ t=1,2,\ n_1,n_2\in\mathbb{N},\ T_1,T_2\in\mathbb{R}^+.$$

Also, the vector of $2D-BPFs$ is as

$$\breve{B}_p(x,y)=[\breve{b_p}^{1,1}(x,y),\cdots,\breve{b_p}^{1,n_1}(x,y),\breve{b_p}^{2,1}(x,y),\cdots,\breve{b_p}^{n_1,n_2}(x,y)]^T. \quad (2)$$

By expanding any bounded square integrable function such as $h(x,y)$ with respect to the $2D-BPFs$ in $L^2[0,T)$, provided that $n_1\to\infty$ and $n_2\to\infty$, we can write

$$h(x,y)\simeq\sum_{i=1}^{n_1}\sum_{j=1}^{n_2}h_{i,j}\breve{b_p}^{i,j}(x,y), \quad (3)$$

where

$$h_{i,j}=\frac{1}{v_1v_2}\int_{(i-1)v_1}^{iv_1}\int_{(j-1)v_2}^{jv_2}h(x,y)dydx. \quad (4)$$

2.2 Chebyshev polynomials

As we know, Chebyshev polynomials are a class of special orthogonal polynomials that are defined in two different types. The first type of these polynomials is defined in the interval $[-1,1]$ and with the weight function $\widetilde{wf}(x)=1\backslash\sqrt{1-x^2}$ as [26]

$$\begin{cases}\widehat{ch}_0^{"1"}(x)=1\\\widehat{ch}_1^{"1"}(x)=x\times\widehat{ch}_0^{"1"}(x)\\\widehat{ch}_n^{"1"}(x)=2x\times\widehat{ch}_{n-1}^{"1"}(x)-\widehat{ch}_{n-2}^{"1"}(x),\quad n\ge2\end{cases}.$$

The trigonometric form of this type of polynomial can also be represented as follows:

$$\widehat{ch}_n^{"1"}(x)=Cos(\theta),\ \ Cos(\theta)=x.$$

But Chebyshev polynomials of the second kind are also introduced in the interval $[-1,1]$ and with the weight function $\widetilde{wf}(x)=\sqrt{1-x^2}$ as

$$\begin{cases}\widehat{ch}_0^{"2"}(x)=1\\\widehat{ch}_1^{"2"}(x)=x\times\widehat{ch}_0^{"2"}(x)\\\widehat{ch}_n^{"2"}(x)=2x\times\widehat{ch}_{n-1}^{"2"}(x)-\widehat{ch}_{n-2}^{"2"}(x),\quad n\ge2\end{cases}, \quad (5)$$

as its trigonometric form is as

$$\widehat{ch}_n^{"2"}(x)=\frac{Sin((n+1)Cos^{-1}(x))}{Sin(Cos^{-1}(x))},\ \ n=0,1,\ldots,$$

that is

$$\widehat{ch}_n^{"2"}(x)=\frac{Sin((n+1)\theta)}{Sin(\theta)},\ \ x=Cos(\theta). \quad (6)$$

2.3 Chebyshev wavelets

As we know the $1D-CWs^{2k}$, which are constructed based on Chebyshev polynomials of the second kind, are defined on $[-1,1]$, for arbitrary natural numbers k and M, as

$$\widehat{cw}_{i,j}(x)=\begin{cases}\frac{2^{0.5k+1}}{\sqrt{\pi}}\widehat{ch}_j^{"2"}(2^{k+1}x-2i-1), & \frac{i}{2^k}\le x\le\frac{i+1}{2^k}\\0, & otherwise\end{cases}, \quad (7)$$

for $i=0,1,\ldots,2^k-1$, and $j=0,1,\ldots,M-1$, so that this set forms a unitary orthogonal basis with respect to the weight functions

$$\begin{cases}\widetilde{wf}_{i,k}(x)=\widetilde{wf}(2^{k+1}x-2i-1)\\\widetilde{wf}(t)=\sqrt{1-t^2}\end{cases},$$

in the space $L^2_{\widetilde{wf}_{i,k}}[0,1]$. The counterpart of the same function in equation (7) for $2D-CWs^{2k}$, on $[-1,1]^2$, for arbitrary natural numbers k_1, k_2, M_1 and M_2,can be written as

$$\widehat{cw}_{i_1,j_1,i_2,j_2}(x,y)$$

https://doi.org/10.57647/mathsci.2025.1902.09

$$= \begin{cases} \dfrac{2^{0.5(k_1+k_2)+2}}{\pi} \widehat{ch}_{j_1}^{"2"}(x_{i_1}^{k_1}) \times \widehat{ch}_{j_2}^{"2"}(y_{i_2}^{k_2}), & \begin{cases} \dfrac{i_1}{2^{k_1}} \le x \le \dfrac{i_1+1}{2^{k_1}} \\ \dfrac{i_2}{2^{k_2}} \le y \le \dfrac{i_2+1}{2^{k_2}} \end{cases} \\ 0, & otherwise \end{cases} \tag{8}$$

where

$$x_{i_1}^{k_1} = 2^{k_1+1}x - 2i_1 - 1, \quad y_{i_2}^{k_2} = 2^{k_2+1}y - 2i_2 - 1,$$

for

$$i_1 = 0, 1, ..., 2^{k_1} - 1, \; i_2 = 0, 1, ..., 2^{k_2} - 1,$$
$$j_1 = 0, 1, ..., M_1 - 1, \; j_2 = 0, 1, ..., M_2 - 1,$$

so that these functions correspondingly produce a unitary orthogonal basis based on the weight functions

$$\begin{cases} \widetilde{wf}_{i_1,k_1,i_2,k_2}(x, y) = \widetilde{wf}(x_{i_1}^{k_1})\widetilde{wf}(y_{i_2}^{k_2}) \\ \widetilde{wf}(s, t) = \sqrt{(1 - s^2)(1 - t^2)} \end{cases}, \tag{9}$$

in the space $L^2_{\widetilde{wf}_{i_1,k_1,i_2,k_2}}[0, 1]^2$.

2.4 Expansion of functions based on Chebyshev wavelets

In this subsection, our goal is to expand suitable bivariate and quadratic functions based on the $2D - CWs^{2k}$, and their unitary orthogonality property. First, we consider a square-integrable bivariate function $h(x, y)$ on $[-1, 1]^2$. This function expands based on the $2D - CWs^{2k}$ defined in (8) with respect to the weight functions defined in (9) at the nodes

$$\frac{i_1}{2^{k_1}} \le x \le \frac{i_1 + 1}{2^{k_1}}, \; \frac{i_2}{2^{k_2}} \le y \le \frac{i_2 + 1}{2^{k_2}},$$

as

$$h(x, y) = \sum_{i_1=0}^{\infty}\sum_{j_1=0}^{\infty}\sum_{i_2=0}^{\infty}\sum_{j_2=0}^{\infty} h_{i_1,j_1,i_2,j_2}\widehat{cw}_{i_1,j_1,i_2,j_2}(x, y), \tag{10}$$

where

$$h_{i_1,j_1,i_2,j_2} =< h(x, y), \widehat{cw}_{i_1,j_1,i_2,j_2}(x, y) >_{\widetilde{wf}_{i_1,k_1,i_2,k_2}}. \tag{11}$$

If we cut the series (10) into sufficiently suitable quantities k_1, k_2, M_1 and M_2, we have

$$\begin{aligned} h(x, y) &= \sum_{i_1=0}^{2^{k_1}-1}\sum_{j_1=0}^{M_1-1}\sum_{i_2=0}^{2^{k_2}-1}\sum_{j_2=0}^{M_2-1} h_{i_1,j_1,i_2,j_2}\widehat{cw}_{i_1,j_1,i_2,j_2}(x, y) \\ &= H^T\widehat{CW}(x, y), \end{aligned} \tag{12}$$

where H and $\widehat{CW}$ are $(\mu = 2^{k_1}M_1 \times 2^{k_2}M_2)$-dimensional column vectors as

$$\begin{aligned} H = [&h_{0,0,0,0}, \ldots, h_{0,M_1-1,2^{k_2}-1,M_2-1}, \\ &\ldots, h_{2^{k_1}-1,M_1-1,2^{k_2}-1,M_2-1}]^T, \end{aligned} \tag{13}$$

and

$$\begin{aligned} \widehat{CW}(x, y) = [&\widehat{cw}_{0,0,0,0}(x, y), \ldots, \\ &\widehat{cw}_{2^{k_1}-1,M_1-1,2^{k_2}-1,M_2-1}(x, y)]^T, \end{aligned} \tag{14}$$

respectively. Now we generalize the same expansion for square-integrable four-variable function $h(x_1, x_2, x_3, x_4)$ on $[-1, 1]^4$, considering the weight functions

$$\begin{cases} \widetilde{wf}_{i_1,k_1,i_2,k_2,i_3,k_3,i_4,k_4}(x_1, x_2, x_3, x_4) \\ \quad = \prod_{a=1}^{4} \widetilde{wf}(2^{k_a+1}x_a - 2i_a - 1) \\ \widetilde{wf}(x_1, x_2, x_3, x_4) = \prod_{a=1}^{4}\sqrt{1 - x_a^2} \end{cases},$$

and at the nodes $\dfrac{i_a}{2^{k_a}} \le x_a \le \dfrac{i_a + 1}{2^{k_a}}$, $a = 1, 2, 3, 4$, so that we arrive at the result

$$\begin{aligned} h(x_1, x_2, x_3, x_4) \simeq &\sum_{i_1=0}^{2^{k_1}-1}\sum_{j_1=0}^{M_1-1}\sum_{i_2=0}^{2^{k_2}-1} \\ &\sum_{j_2=0}^{M_2-1}\sum_{i_3=0}^{2^{k_3}-1}\sum_{j_3=0}^{M_3-1}\sum_{i_4=0}^{2^{k_4}-1}\sum_{j_4=0}^{M_4-1} h_{i_1,j_1,i_2,j_2,i_3,j_3,i_4,j_4} \\ &\times\widehat{cw}_{i_1,j_1,i_2,j_2,i_3,j_3,i_4,j_4}(x_1, x_2, x_3, x_4) \\ &= \widehat{CW}^T(x_1, x_2) \times H \times \widehat{CW}(x_3, x_4) \\ &= \widehat{CW}^T(x_3, x_4) \times H^T \times \widehat{CW}(x_1, x_2). \end{aligned} \tag{15}$$

So that each of the vectors $\widehat{CW}(x_1, x_2)$ and $\widehat{CW}(x_3, x_4)$ are the μ-dimensional vectors defined in (14) and for the matrix of coefficients H we have

$$H = [h_{i_1,j_1,i_2,j_2,i_3,j_3,i_4,j_4}]_{\mu\times\mu}, \tag{16}$$

with

$$\begin{aligned} h_{i_1,j_1,i_2,j_2,i_3,j_3,i_4,j_4} &=< h(x_1, x_2, x_3, x_4), \\ \widehat{cw}_{i_1,j_1,i_2,j_2,i_3,j_3,i_4,j_4}(x_1, x_2, x_3, x_4) &>_{\widetilde{wf}_{i_1,k_1,i_2,k_2,i_3,j_3,i_4,j_4}}. \end{aligned} \tag{17}$$

2.5 Chebyshev wavelets based on block pulse functions

To organize our numerical method, we need to obtain a relation between the $2D-CWs^{2k}$ and the $2D-BPFs$, so that we can use this relation to calculate the $2D-CWs^{2k}$ operational matrices in the next section. To do this, we prove the following theorem.

Theorem 2.1 *We consider the vector the $2D - CWs^{2k}$ of $\widehat{CW}(x, y)$ and the $2D - BPFs$ of $\breve{B}_p(x, y)$ defined in equations (14) and (2), respectively. If we expand the $\widehat{CW}(x, y)$ based on the $\breve{B}_p(x, y)$, we have*

$$\widehat{CW}(x, y) = \Lambda\breve{B}_p(x, y),$$

where Λ is an $(\mu \times \mu)$-dimensional matrix in form

$$\begin{aligned} \Lambda &= [\Lambda_{i_1,j_1,i_2,j_2}] \\ &= \left[\widehat{cw}_{i_1,j_1,i_2,j_2}\left(\frac{2i_1 - 1}{2(2^{k_1} - 1)(M_1 - 1)}, \right.\right. \\ &\qquad \left.\left.\frac{2i_2 - 1}{2(2^{k_2} - 1)(M_2 - 1)}\right)\right], \end{aligned}$$

with

$$i_1, j_1 = 0, 1, ..., (2^{k_1} - 1)(M_1 - 1),$$
$$i_2, j_2 = 0, 1, ..., (2^{k_2} - 1)(M_2 - 1).$$

https://doi.org/10.57647/mathsci.2025.1902.09

Proof. Based on Eq. (3) and by expanding the (i_1, j_1, i_2, j_2)th member of the vector $\widehat{CW}(x, y)$ with respect to the $2D - BPFs$, for $i_1, j_1 = 0, 1, ..., (2^{k_1} - 1)(M_1 - 1)$, $i_2, j_2 = 0, 1, ..., (2^{k_2} - 1)(M_2 - 1)$ we have

$$\widehat{cw}_{i_1,j_1,i_2,j_2}(x, y) = \sum_{i_1=0}^{(2^{k_1}-1)(M_1-1)} \sum_{i_2=0}^{(2^{k_2}-1)(M_2-1)} \Lambda_{i_1,j_1,i_2,j_2} \breve{b}_p^{\,i_1,i_2}(x, y).$$

On the other hand, according to Eq. (4), we get

$$\Lambda_{i_1,j_1,i_2,j_2} = (2^{k_1}-1)(M_1-1)(2^{k_2}-1)(M_2-1) \times \int_{(i_2-1)/(2^{k_2}-1)(M_2-1)}^{i_2/(2^{k_2}-1)(M_2-1)} \int_{(i_1-1)/(2^{k_1}-1)(M_1-1)}^{i_1/(2^{k_1}-1)(M_1-1)} \widehat{cw}_{i_1,j_1,i_2,j_2}(x, y)dxdy. \quad (18)$$

From the mean value theorem we can see Eq. (18) as

$$\begin{aligned}\Lambda_{i_1,j_1,i_2,j_2} &= (2^{k_1} - 1)(M_1 - 1)(2^{k_2} - 1)(M_2 - 1) \\ &\times \int_{(i_2-1)/(2^{k_2}-1)(M_2-1)}^{i_2/(2^{k_2}-1)(M_2-1)} \frac{1}{(2^{k_1} - 1)(M_1 - 1)} \\ &\quad \times \widehat{cw}_{i_1,j_1,i_2,j_2}(\eta_{i_1}, y)dxdy \\ &= (2^{k_2} - 1)(M_2 - 1)\frac{1}{(2^{k_2} - 1)(M_2 - 1)} \\ &\quad \times \widehat{cw}_{i_1,j_1,i_2,j_2}(\eta_{i_1}, \eta_{i_2}),\end{aligned}$$

where η_{i_1} and η_{i_2} are actually the averages of intervals

$$\left(\frac{i_1 - 1}{(2^{k_1} - 1)(M_1 - 1)}, \frac{i_1}{(2^{k_1} - 1)(M_1 - 1)}\right),$$

and

$$\left(\frac{i_2 - 1}{(2^{k_2} - 1)(M_2 - 1)}, \frac{i_2}{(2^{k_2} - 1)(M_2 - 1)}\right),$$

respectively, so we get

$$\Lambda_{i_1,j_1,i_2,j_2} = \widehat{cw}_{i_1,j_1,i_2,j_2}\left(\frac{2i_1 - 1}{(2^{k_1} - 1)(M_1 - 1)}, \frac{2i_2 - 1}{(2^{k_2} - 1)(M_2 - 1)}\right).$$

The proof is complete. □

We conclude this section with two fundamental points that are of great importance for explaining our numerical method.

Point 1. Considering the $2D - CWs^{2k}$, for any μ-dimension vector H we always have

$$\widehat{CW}(x, y)\widehat{CW}^T(x, y)H = \ddot{H}\widehat{CW}(x, y),$$

where

$$\ddot{H}_{\mu\times\mu} = \Lambda_{\mu\times\mu}\dot{H}\Lambda^{-1}_{\mu\times\mu},$$

with

$$\dot{H}_{\mu\times\mu} = diag(\Lambda^T_{\mu\times\mu}H_{\mu\times1}),$$

where Λ is defined in Theorem 2.1.

Point 2. Considering the $2D - CWs^{2k}$, for any $(\mu \times \mu)$-dimension matrix J we always have

$$\widehat{CW}^T(x, y)J\widehat{CW}(x, y) = \ddot{J}^T\widehat{CW}(x, y),$$

where

$$\ddot{J} = \grave{J}^T\Lambda^{-1},$$

with

$$\grave{J}_{\mu\times1} = diag(\Lambda^T J\Lambda).$$

3. Calculation of operational matrices

In this section, we first introduce the operational matrices of the $2D - BPFs$ by the presented lemmas [9], and then, with the help of these lemmas and the governing relations between $2D - CWs^{2k}$ and $2D - BPFs$, we obtain the operational matrices of $2D - CWs^{2k}$. We also remind you that in this section, the symbol $\otimes$ refers to the Kronecker multiplication.

Lemma 3.1 *According to the definition of $2D - BPFs$, by considering*

$$n_1 = 2^{k_1},\ n_2 = M_1,$$

we can obtain the ordinary Volterra operational matrix by the double Volterra and ordinary integral

$$\int_0^y \int_0^x \breve{B}_p(x, y)(s, t)dsdt = \overline{Oo}\breve{B}_p(x, y),$$

where

$$\overline{Oo} = \overline{Mo}_1 \otimes \overline{Mo}_2,$$

such that $\overline{Mo}_1$ and $\overline{Mo}_2$ are the $(n_1 \times n_2)$-dimensional ordinary operational matrices of $1D - BPFs$ as

$$\overline{Mo}_a = \frac{1}{2n_a}\begin{pmatrix} 1 & 2 & 2 & \dots & 2 \\ 0 & 1 & 2 & \dots & 2 \\ 0 & 0 & 1 & \dots & \vdots \\ \vdots & \vdots & \vdots & \ddots & \vdots \\ 0 & 0 & 0 & \dots & 1 \end{pmatrix},\ a = 1, 2.$$

Lemma 3.2 *According to the definition of $2D - BPFs$, by considering*

$$n_1 = 2^{k_1},\ n_2 = M_1,$$

we can obtain the stochastic Volterra operational matrix by the double Volterra and stochastic integrals

$$\int_0^y \int_0^x \breve{B}_p(x, y)(s, t)dB_a(s)dB_b(s) = \overline{Os}_{a,b}\breve{B}_p(x, y),$$

where

$$\overline{Os}_{a,b} = \overline{Ms}_1^a \otimes \overline{Ms}_2^b,$$

for $a = 1, 2, \dots, \iota_1$ and $b = 1, 2, \dots, \iota_2$, such that $\overline{Ms}_1^a$ and $\overline{Ms}_2^b$ are the $(n_1 \times n_2)$-dimensional stochastic operational matrices of $1D - BPFs$ as

$$\overline{Ms}_i^j = \begin{pmatrix} B_j(\frac{v_i}{2}) & B_j(v_i) & \dots & B_j(v_i) \\ 0 & B_j(\frac{3v_i}{2}) - B_j(v_i) & \dots & B_j(2v_i) - B_j(v_i) \\ 0 & 0 & \dots & B_j(3v_i) - B_j(2v_i) \\ \vdots & \vdots & \ddots & \vdots \\ 0 & 0 & \dots & B_j(\frac{(2n_i-1)v_i}{2}) - B_j((n_i-1)v_i) \end{pmatrix},$$

for $i = 1, 2$ and $j = a, b$.

3.1 Ordinary Fredholm Chebyshev operational matrix

In this subsection, we obtain the ordinary Fredholm operational matrix of the $2D-CWs^{2k}$. This is achieved by considering the definition of these wavelets in Eq. (8) and on the basis that the $2D - CWs^{2k}$ are orthonormal. So for the following ordinary Fredholm double integral, we have

$$\int_0^1 \int_0^1 \widehat{CW}(s,t)\widehat{CW}^T(s,t)dsdt = F_O, \qquad (19)$$

where $(F_O)_{\mu\times\mu}$ is the Identity matrix.

3.2 Ordinary Volterra Chebyshev operational matrix

In this subsection, we derive the ordinary Volterra operational matrix for the $2D - CWs^{2k}$ by presenting the following theorem.

Theorem 3.3 *If we take the ordinary double integral of the Volterra type of the vector of the $2D - CWs^{2k}$, we get*

$$\int_0^y \int_0^x \widehat{CW}(s,t)dsdt = V_O \times \widehat{CW}(x,y),$$

which V_O is called the ordinary Volterra operational matrix attributed to the $2D - CWs^{2k}$.

Proof. Using Theorem 2.1 we can write

$$\begin{aligned} \int_0^y \int_0^x \widehat{CW}(s,t)dsdt &= \int_0^y \int_0^x \Lambda \breve{B}_p(s,t)dsdt \\ &= \Lambda \times \overline{Oo} \times \breve{B}_p(x,y), \\ &= \Lambda \times \overline{Oo} \times (\Lambda^{-1}\widehat{CW}(x,y)) \\ &= V_O \times \widehat{CW}(x,y), \end{aligned}$$

where

$$V_O = \Lambda \times \overline{Oo} \times \Lambda^{-1},$$

and Λ and $\overline{Oo}$ are defined in Theorem 2.1 and Lemma 3.1, respectively. The proof is complete. □

3.3 Stochastic Volterra Chebyshev operational matrix

In this subsection, we discuss how to calculate the stochastic operational matrices from the stochastic integrals of the $2D-CWs^{2k}$, which results in the following theorem.

Theorem 3.4 *If we take the stochastic double integrals of the Volterra type of the vector of the $2D-CWs^{2k}$, we get*

$$\int_0^y \int_0^x \widehat{CW}(s,t)dB_a(s)dB_b(t) = \overline{VS}_{a,b} \times \widehat{CW}(x,y),$$

which $\overline{VS}_{a,b}$ are called the stochastic Volterra operational matrices attributed to the $2D - CWs^{2k}$, for $a = 1, 2, ..., t_1$ and $b = 1, 2, ..., t_2$.

Proof. Using Theorem 2.1 we can write

$$\begin{aligned} &\int_0^y \int_0^x \widehat{CW}(s,t)dB_a(s)dB_b(t) \\ &= \int_0^y \int_0^x \Lambda \breve{B}_p(s,t)dB_a(s)dB_b(t) \\ &= \Lambda \times \overline{Os}_{a,b} \times \breve{B}_p(x,y) \\ = \ &\Lambda \overline{Os}_{a,b}(\Lambda^{-1}\widehat{CW}(x,y)) \\ &= \overline{VS}_{a,b}\widehat{CW}(x,y), \end{aligned}$$

where

$$\overline{VS}_{a,b} = \Lambda\, \overline{Os}_{a,b}\, \Lambda^{-1},$$

and Λ and $\overline{Os}_{a,b}$ are defined in Theorem 2.1 and Lemma 3.2, respectively. The proof is complete. □

4. Chebyshev numerical method

In this section, considering the results obtained from the previous sections of this paper, we solve Eq. (1) numerically. First, we rewrite the functions appearing in this equation in terms of the $2D - CWs^{2k}$ in the following vector forms.

$$f(x,y) = F^T\widehat{CW}(x,y) = \widehat{CW}^T(x,y)F, \qquad (20)$$

$$g(x,y) = G^T\widehat{CW}(x,y) = \widehat{CW}^T(x,y)G, \qquad (21)$$

and

$$\begin{aligned} u_i(x,y,s,t) &= \widehat{CW}^T(x,y)U_i^T\widehat{CW}(s,t) \qquad (22) \\ &= \widehat{CW}^T(s,t)U_i\widehat{CW}(x,y), \end{aligned}$$

https://doi.org/10.57647/mathsci.2025.1902.09

for $i = 1, 2, 3$. After applying the last three relations to Eq. (1), we get

$$\begin{aligned}
&G^T\widehat{CW}(x,y) = F^T\widehat{CW}(x,y)\\
&+\int_0^1\int_0^1 \widehat{CW}^T(x,y)U_1^T\widehat{CW}(s,t)\widehat{CW}^T(s,t)Gdsdt\\
&+\int_0^y\int_0^x \widehat{CW}^T(x,y)U_2^T\widehat{CW}(s,t)\widehat{CW}^T(s,t)Gdsdt\\
&+\sum_{a=1}^{\iota_1}\sum_{b=1}^{\iota_2}\int_0^y\int_0^x \widehat{CW}^T(x,y)U_3^T\widehat{CW}(s,t)\\
&\times\widehat{CW}^T(s,t)GdB_a(s)dB_b(t) = F^T\widehat{CW}(x,y)\\
&+\widehat{CW}^T(x,y)U_1^T\left(\int_0^1\int_0^1 \widehat{CW}(s,t)\widehat{CW}^T(s,t)dsdt\right)G\\
&+\widehat{CW}^T(x,y)U_2^T\int_0^y\int_0^x \widehat{CW}(s,t)\widehat{CW}^T(s,t)Gdsdt\\
&+\sum_{a=1}^{\iota_1}\sum_{b=1}^{\iota_2}\widehat{CW}^T(x,y)U_3^T\int_0^y\int_0^x \widehat{CW}(s,t)\widehat{CW}^T\\
&\quad(s,t)GdB_a(s)dB_b(t).
\end{aligned}$$

Comparing the last relation, Point (1) and Eq. (19), we have

$$\begin{aligned}
&G^T\widehat{CW}(x,y) = F^T\widehat{CW}(x,y) + \widehat{CW}^T(x,y)U_1^TF_OG\\
&+\widehat{CW}^T(x,y)U_2^T\int_0^y\int_0^x \ddot{G}\widehat{CW}(s,t)dsdt\\
&+\sum_{a=1}^{\iota_1}\sum_{b=1}^{\iota_2}\widehat{CW}^T(x,y)U_3^T\int_0^y\int_0^x \ddot{G}\widehat{CW}(s,t)dB_a(s)dB_b(t).
\end{aligned}$$

Now it is the turn to use Theorems 3.3 and 3.4, that by applying these two theorems to the last relation we have

$$\begin{aligned}
&[G^T\widehat{CW}(x,y) = F^T\widehat{CW}(x,y) + \widehat{CW}^T(x,y)U_1^TF_OG\\
&+\widehat{CW}^T(x,y)U_2^T\ddot{G}V_O\widehat{CW}(x,y)\\
&+\sum_{a=1}^{\iota_1}\sum_{b=1}^{\iota_2}\widehat{CW}^T(x,y)U_3^T\ddot{G}\overline{VS}_{a,b}\widehat{CW}(x,y).
\end{aligned}$$

Relation (21) and point 2 lead us to the relation

$$\begin{aligned}
&G^T\widehat{CW}(x,y) = F^T\widehat{CW}(x,y) + G^TF_O^TU_1\widehat{CW}(x,y)\\
&+\ddot{J_O}^T\widehat{CW}(x,y) + \sum_{a=1}^{\iota_1}\sum_{b=1}^{\iota_2}(\ddot{J_S})_{a,b}^T\widehat{CW}(x,y), \qquad (23)
\end{aligned}$$

where

$$\ddot{J_O} = \dot{J_O}^T\Lambda^{-1},\ \ (\ddot{J_S})_{a,b}^T = (\dot{J_S})_{a,b}^T\Lambda^{-1}, \qquad (24)$$

with

$$\begin{aligned}
\dot{J_O} &= diag(\Lambda^TU_2^T\ddot{G}V_O\Lambda),\ (\dot{J_S})_{a,b}\\
&= diag(\Lambda^TU_3^T\ddot{G}\overline{VS}_{a,b}\Lambda). \qquad (25)
\end{aligned}$$

Now, simplifying Eq. (23), it leads to the linear system

$$G^T = F^T + R^T + \ddot{J_O}^T + \sum_{a=1}^{\iota_1}\sum_{b=1}^{\iota_2}(\ddot{J_S})_{a,b}^T, \qquad (26)$$

where

$$R = U_1^TF_OG. \qquad (27)$$

Finally, after solving the linear system of μ equations and μ unknowns, which is done using special methods for such systems, the solution vector $G(x,y)$ is obtained, which by substituting into Eq. (21), we can calculate the value of the solution of Eq. (1) at any desired point.

5. Convergence and error checking

In this section, after examining the convergence of the two and four-variable functions expanded with respect to the $2D - CWs^{2k}$, we analyze the error of our new method for solving Eq. (1). In this direction, we present the following important and fundamental theorems.

Theorem 5.1 *For a function $h(x,y) \in \widetilde{L^2_{wf}}[0,1)^2$ with a bounded fourth derivative of the form $\left|\frac{\partial^4 h}{\partial x^2\partial y^2}\right| \le \lambda_1$, the $2D - CWs^{2k}$ expansion*

$$\dot{h}(x,y) = \sum_{i_1=0}^{2^{k_1}-1}\sum_{j_1=0}^{M_1-1}\sum_{i_2=0}^{2^{k_2}-1}\sum_{j_2=0}^{M_2-1} h_{i_1,j_1,i_2,j_2}\widehat{cw}_{i_1,j_1,i_2,j_2}(x,y),$$

converges uniformly to the function $h(x,y)$, which means

$$\left\|h(x,y) - \dot{h}(x,y)\right\|_2 \le \gamma_1,$$

where λ_1 and γ_1 are the real constants.

Proof. Considering the $2D - CWs^{2k}$ expansion $\dot{h}(x,y)$ and combining relations (8), (9), and (11), we have

$$\begin{aligned}
h_{i_1,j_1,i_2,j_2} &= \frac{2^{0.5(k_1+k_2)+2}}{\pi}\int_{i_2/2^{k_2}}^{(i_2+1)/2^{k_2}}\int_{i_1/2^{k_1}}^{(i_1+1)/2^{k_1}}\\
&h(x,y)\widehat{ch}_{j_1}^{"2"}(2^{k_1+1}x - 2i_1 - 1)\\
&\times\widehat{ch}_{j_2}^{"2"}(2^{k_2+1}y - 2i_2 - 1)\widetilde{wf}(2^{k_1+1}x - 2i_1 - 1)\\
&\times\widetilde{wf}(2^{k_2+1}y - 2i_2 - 1)dxdy.
\end{aligned}$$

By separating the integrals, we get

$$\begin{aligned}
h_{i_1,j_1,i_2,j_2} &= \frac{2^{0.5(k_1+k_2)+2}}{\pi}\\
&\times\int_{i_2/2^{k_2}}^{(i_2+1)/2^{k_2}}\widehat{ch}_{j_2}^{"2"}(2^{k_2+1}y - 2i_2 - 1)\\
&\times\widetilde{wf}(2^{k_2+1}y - 2i_2 - 1)\tilde{I}(x)dy, \qquad (28)
\end{aligned}$$

where

$$\begin{aligned}
\tilde{I}(x) &= \int_{i_1/2^{k_1}}^{(i_1+1)/2^{k_1}} h(x,y)\widehat{ch}_{j_1}^{"2"}(2^{k_1+1}x - 2i_1 - 1)\\
&\times\widetilde{wf}(2^{k_1+1}x - 2i_1 - 1)dx.
\end{aligned}$$

To solve the integral $\tilde{I}(x)$, using Eq. (6), we can consider

$$2^{k_1+1}x - 2i_1 - 1 = Cos(\theta_1),$$

https://doi.org/10.57647/mathsci.2025.1902.09

therefore we have

$$x = \frac{Cos(\theta_1) + 2i_1 + 1}{2^{k_1+1}} \Rightarrow \begin{cases} x = i_1/2^{k_1} \to \theta_1 = \pi \\ x = (i_1+1)/2^{k_1+1} \to \theta_1 = 0 \end{cases}, \quad (29)$$

now, using Eq. (29), defining the weight function $\widetilde{wf}$ in Subsection 2.3, and applying the change of variable method to the integral $\tilde{I}(x)$, we conclude

$$\tilde{I}(x) = \int_0^{\pi} h\left(\frac{\cos(\theta_1) + 2i_1 + 1}{2^{k_1+1}}, y\right) \times \sin((n+1)\theta_1)\sin(\theta_1)d\theta_1. \quad (30)$$

By applying relation

$$Sin(a)Sin(b) = \frac{1}{2}[Cos(a-b) - Cos(a+b)],$$

to Eq. (30), we obtain

$$\tilde{I}(x) = \int_0^{\pi} h\left(\frac{Cos(\theta_1) + 2i_1 + 1}{2^{k_1+1}}, y\right) \times [Cos(n\theta_1) - Cos((n+2)\theta_1)]\, d\theta_1. \quad (31)$$

Using the method of integration by parts

$$\begin{cases} u = h\left(\frac{Cos(\theta_1) + 2i_1 + 1}{2^{k_1+1}}, y\right) \\ u_x = \frac{\partial h}{\partial x}\left(\frac{Cos(\theta_1) + 2i_1 + 1}{2^{k_1+1}}, y\right)\frac{-Sin(\theta_1)}{2^{k_1+1}}d\theta_1 \end{cases},$$

and

$$\begin{cases} dv = [Cos(n\theta_1) - Cos((n+2)\theta_1)]\, d\theta_1 \\ v = \frac{1}{n}Sin(n\theta_1) - \frac{1}{n+2}Sin((n+2)\theta_1) \end{cases},$$

in Eq. (31), and also considering the limits of integration of $[0, \pi]$ in this equation we get

$$\tilde{I}(x) = \frac{1}{2^{k_1+2}}\int_0^{\pi}\left(\frac{1}{n+2}Sin((n+2)\theta_1) - \frac{1}{n}Sin(n\theta_1)\right) \times \frac{\partial h}{\partial x}\left(\frac{Cos(\theta_1) + 2i_1 + 1}{2^{k_1+1}}, y\right)d\theta_1. \quad (32)$$

We use integration by parts once again, changing the variable

$$\begin{cases} u = \frac{\partial h}{\partial x}\left(\frac{Cos(\theta_1) + 2i_1 + 1}{2^{k_1+1}}, y\right) \\ dv = \left(\frac{1}{n+2}Sin((n+2)\theta_1) - \frac{1}{n}Sin(n\theta_1)\right)d\theta_1 \end{cases},$$

thus, Eq. (32) becomes:

$$\tilde{I}(x) = \frac{1}{2^{k_1+3}}\int_0^{\pi}\frac{\partial^2 h}{\partial x^2}\left(\frac{Cos(\theta_1)+2i_1+1}{2^{k_1+1}}, y\right)\overline{A}(n,\theta_1)d\theta_1, \quad (33)$$

where

$$\overline{A}(n,\theta_1) = \frac{Sin(\theta_1)}{2n}\left(\frac{Sin((n-1)\theta_1)}{n-1} - \frac{Sin((n+1)\theta_1)}{n+1}\right) - \frac{Sin(\theta_1)}{2(n+2)}\left(\frac{Sin((n+1)\theta_1)}{n+1} - \frac{Sin((n+3)\theta_1)}{n+3}\right).$$

Now, by substituting Eq. (33) into Eq. (23) and repeating a process similar to steps (29) to (33), we obtain

$$h_{i_1,j_1,i_2,j_2} = \frac{2^{0.5(k_1+k_2)+2}}{\pi} \times \frac{1}{2^{k_2+3}} \times \frac{1}{2^{k_1+3}}\int_0^{\pi}\int_0^{\pi} \overline{A}(n,\theta_1)\overline{A}(n,\theta_2) \times \frac{\partial^4 h}{\partial x^2 \partial y^2}\left(\frac{Cos(\theta_1)+2i_1+1}{2^{k_1+1}}, \frac{\cos(\theta_2)+2i_2+1}{2^{k_2+1}}\right)d\theta_1 d\theta_2, \quad (34)$$

where

$$\overline{A}(n,\theta_2) = \frac{Sin(\theta_2)}{2n}\left(\frac{Sin((n-1)\theta_2)}{n-1} - \frac{Sin((n+1)\theta_2)}{n+1}\right) - \frac{Sin(\theta_2)}{2(n+2)}\left(\frac{Sin((n+1)\theta_2)}{n+1} - \frac{Sin((n+3)\theta_2)}{n+3}\right).$$

Considering the absolute value for Eq. (34) and also placing the bound of the fourth derivative for the function $h(x, y)$ according to the hypothesis of the theorem, we have

$$\left|h_{i_1,j_1,i_2,j_2}\right| \le \frac{\lambda_1}{\pi \times 2^{1.5(k_1+k_2)+4}}\int_0^{\pi}\int_0^{\pi}\left|\overline{A}(n,\theta_1)\right| \times \left|\overline{A}(n,\theta_2)\right| d\theta_1 d\theta_2. \quad (35)$$

Considering inequality $|Sin(\theta_i)| \le 1$, $i = 1, 2$, and after simplifying expressions $\overline{A}(n,\theta_1)$ and $\overline{A}(n,\theta_2)$, then substituting them into Eq. (35), and finally calculating the double integral (35), we conclude that

$$\left|h_{i_1,j_1,i_2,j_2}\right| \le \frac{\pi\lambda_1}{2^{1.5(k_1+k_2)+4}} \times \frac{1}{(n^2+2n-3)^2}, \quad (36)$$

on the one hand, we know that

$$\begin{cases} i_1 \le 2^{k_1} - 1 \to i_1 + 1 \le 2^{k_1} \to \frac{1}{2^{1.5k_1}} \le \frac{1}{(i_1+1)^{1.5}} \\ i_2 \le 2^{k_2} - 1 \to i_2 + 1 \le 2^{k_2} \to \frac{1}{2^{1.5k_2}} \le \frac{1}{(i_2+1)^{1.5}} \end{cases}, \quad (37)$$

by applying (37) in (36) we obtain

$$\left|h_{i_1,j_1,i_2,j_2}\right| \le \frac{\pi\lambda_1}{16\sqrt{[(i_1+1)(i_2+1)]^3}(n^2+2n-3)^2},$$

This clearly shows that the $2D - CWs^{2k}$ series

$$\sum_{i_1=0}^{\infty}\sum_{j_1=0}^{\infty}\sum_{i_2=0}^{\infty}\sum_{j_2=0}^{\infty} h_{i_1,j_1,i_2,j_2}\widehat{cw}_{i_1,j_1,i_2,j_2}(x,y),$$

converges to the function $h(x, y)$, that is,

$$\left\|h(x,y) - \dot{h}(x,y)\right\|_2 \le \gamma_1.$$

The proof is complete. □

https://doi.org/10.57647/mathsci.2025.1902.09

Theorem 5.2 *For a function* $h(x,y,s,t) \in L^2_{\widetilde{wf}}[0,1)^4$ *with a bounded eighth derivative of the form* $\left|\frac{\partial^8 h}{\partial x^2 \partial y^2 \partial s^2 \partial t^2}\right| \le \lambda_2$, *the* $2D-CWs^{2k}$ *expansion*

$$\dot{h}(x,y,s,t) = \sum_{i_1=0}^{2^{k_1}-1}\sum_{j_1=0}^{M_1-1}\sum_{i_2=0}^{2^{k_2}-1}\sum_{j_2=0}^{M_2-1}\sum_{i_3=0}^{2^{k_3}-1}\sum_{j_3=0}^{M_3-1}\sum_{i_4=0}^{2^{k_4}-1}\sum_{j_4=0}^{M_4-1} h_{i_1,j_1,i_2,j_2,i_3,j_3,i_4,j_4}\widehat{cw}_{i_1,j_1,i_2,j_2,i_3,j_3,i_4,j_4}(x,y,s,t),$$

converges uniformly to the function $h(x,y,s,t)$, *which means*

$$\left\|h(x,y,s,t) - \dot{h}(x,y,s,t)\right\|_2 \le \gamma_2,$$

where λ_2 *and* γ_2 *are the real constants.*

Proof. If we do the same process as Eqs. (28) to (37), this time for the four-variable function $h(x,y,s,t)$, then the uniform convergence of $\dot{h}(x,y,s,t)$ clearly results, so that we can write

$$\left\|h(x,y,s,t) - \dot{h}(x,y,s,t)\right\|_2 \le \gamma_2.$$

The proof is complete. □

Theorem 5.3 *By calling* $g(x,y)$ *and* $\dot{g}(x,y)$ *as the analytical and approximate solutions of Eq.* (1) *based on the* $2D-CWs^{2k}$, *respectively, which are obtained by combining Eqs.* (21) *and* (26), *and also by accepting Assumptions*

(1) $\|g(x,y)\|_2 \le \Gamma,\ (x,y)\in[0,1]^2$,
(2) $\|u_i(x,y,s,t)\|_2 \le \mho_i,\ i=1,2,3,\ (x,y,s,t)\in[0,1]^4$,
(3) $0 \le x,y \le 1 \Rightarrow |x|\le 1,\ |y|\le 1$,
(4) $\Upsilon_i(z) = \sup_{0\le z\le 1}|B_i(z)| < \infty,\ i=1,2,\ldots,\iota_1$, *[2]*
(5) $\Upsilon_j(z) = \sup_{0\le z\le 1}|B_j(z)| < \infty,\ j=1,2,\ldots,\iota_2$, *[2]*
(6) $\left[\mho_1+\mho_2+(\gamma_2)_1+(\gamma_2)_2+\sum_{i=1}^{\iota_1}\sum_{j=1}^{\iota_2}\Upsilon_i(x)\Upsilon_j(y)(\mho_3+(\gamma_2)_3)\right] < 1$,

then the error estimate of the $2D-CWs^{2k}$ *method for solving Eq.* (1) *is as*

$$\|g(x,y)-\dot{g}(x,y)\|_2 \le \frac{\gamma_1+\Gamma\left[(\gamma_2)_1+(\gamma_2)_2+\sum_{i=1}^{\iota_1}\sum_{j=1}^{\iota_2}\Upsilon_i(x)\Upsilon_j(y)(\gamma_2)_3\right]}{1-\left[\mho_1+\mho_2+(\gamma_2)_1+(\gamma_2)_2+\sum_{i=1}^{\iota_1}\sum_{j=1}^{\iota_2}\Upsilon_i(x)\Upsilon_j(y)(\mho_3+(\gamma_2)_3)\right]}.$$

Proof. To check the error of our method, we first consider the difference between each function in Eq. (1) and its approximation in this equation, which we have

$$\begin{aligned} g(x,y)-\dot{g}(x,y) &= f(x,y)-\dot{f}(x,y)\\ &+\int_0^1\int_0^1 [u_1(x,y,s,t)g(s,t)-\dot{u}_1(x,y,s,t)\dot{g}(s,t)]\,dsdt\\ &+\int_0^y\int_0^x [u_2(x,y,s,t)g(s,t)-\dot{u}_2(x,y,s,t)\dot{g}(s,t)]\,dsdt\\ &+\sum_{i=1}^{\iota_1}\sum_{j=1}^{\iota_2}\int_0^y\int_0^x [u_3(x,y,s,t)g(s,t)\\ &\qquad -\dot{u}_3(x,y,s,t)\dot{g}(s,t)]\,dB_i(s)dB_j(t), \end{aligned}$$

clearly the mean value theorem in $(x,y)\in[0,1]^2$ and $(x,y,s,t)\in[0,1]^4$ gives the result that

$$\begin{aligned} \|g-\dot{g}\|_2 &\le \|f-\dot{f}\|_2+\|u_1g-\dot{u}_1\dot{g}\|_2 \\ &\quad +xy\|u_2g-\dot{u}_2\dot{g}\|_2 \\ &\quad +\sum_{i=1}^{\iota_1}\sum_{j=1}^{\iota_2}B_i(x)B_j(y)\|u_3g-\dot{u}_3\dot{g}\|_2. \end{aligned} \tag{38}$$

To obtain the upper bounds of the norms of $\|u_ig-\dot{u}_i\dot{g}\|_2$, $i=1,2,3$, it is sufficient to apply Hypotheses 1 and 2 as well as Theorem 5.2 to each of these norms, which leads to

$$\begin{aligned} \|u_ig-\dot{u}_i\dot{g}\|_2 &\le \|u_i\|_2\|g-\dot{g}\|_2 \\ &\quad +\|u_i-\dot{u}_i\|_2(\|g-\dot{g}\|_2+\|g\|_2) \\ &\le \mho_i\|g-\dot{g}\|_2+(\gamma_2)_i(\|g-\dot{g}\|_2+\Gamma) \\ &= (\mho_i+(\gamma_2)_i)\|g-\dot{g}\|_2+(\gamma_2)_i\Gamma. \end{aligned} \tag{39}$$

Substituting the Eq. (39) into (38) and using Theorem 5.1, we get

$$\begin{aligned} &\|g-\dot{g}\|_2 \le \gamma_1+(\mho_1+(\gamma_2)_1)\|g-\dot{g}\|_2+(\gamma_2)_1\Gamma \\ &+xy\left[(\mho_2+(\gamma_2)_2)\|g-\dot{g}\|_2+(\gamma_2)_2\Gamma\right] \\ &+\sum_{i=1}^{\iota_1}\sum_{j=1}^{\iota_2}B_i(x)B_j(y)\left[(\mho_3+(\gamma_2)_3)\|g-\dot{g}\|_2+(\gamma_2)_3\Gamma\right]. \end{aligned} \tag{40}$$

Now if we consider the right-hand supremum of Eq. (40) and also apply Hypotheses 3, 4 and 5, we have

$$\begin{aligned} &\|g-\dot{g}\|_2 \le \gamma_1 \\ &+(\mho_1+\mho_2+(\gamma_2)_1+(\gamma_2)_2)\sup_{0\le x,y\le 1}\|g-\dot{g}\|_2 \\ &+(\gamma_2)_1\Gamma+(\gamma_2)_2\Gamma+\sum_{i=1}^{\iota_1}\sum_{j=1}^{\iota_2}\Upsilon_i(x)\Upsilon_j(y) \\ &\times\left[(\mho_3+(\gamma_2)_3)\sup_{0\le x,y\le 1}\|g-\dot{g}\|_2+(\gamma_2)_3\Gamma\right], \end{aligned}$$

finally, provided that Hypothesis 6 is established, the error estimate of the $2D-CWs^{2k}$ method is obtained as

$$\|g(x,y)-\dot{g}(x,y)\|_2 \le \frac{\gamma_1+\Gamma\left[(\gamma_2)_1+(\gamma_2)_2+\sum_{i=1}^{\iota_1}\sum_{j=1}^{\iota_2}\Upsilon_i(x)\Upsilon_j(y)(\gamma_2)_3\right]}{1-\left[\mho_1+\mho_2+(\gamma_2)_1+(\gamma_2)_2+\sum_{i=1}^{\iota_1}\sum_{j=1}^{\iota_2}\Upsilon_i(x)\Upsilon_j(y)(\mho_3+(\gamma_2)_3)\right]}.$$

The proof is complete. □

5.1 Algorithm of 2D cLP-BPfs combination method

In this subsection, we describe the algorithm of the method used in this article. All our calculations are based on this algorithm using Mathematica Wolfram 12 software, so that for each example, for at least 250 turns, this algorithm has been implemented to build a confidence interval for the approximate solutions.

Input: k_1, k_2, M_1, M_2, T_1, T_2, ι_1, ι_2, ..., $\underline{B_i(t)}(1 \le i \le \iota_1)$, $B_j(t)(1 \le j \le \iota_2)$, $\underline{Mo_1}$, $\underline{Mo_2}$, $\underline{Ms_1^a}(a =$

$1, 2, ..., \iota_1$), $\overline{Ms}_2^b (b = 1, 2, ..., \iota_2)$, f and $u_i (i = 1, 2, 3)$.
Step 1: Define the Chebyshev polynomials of the second kind from Eq. (5).
Step 2: Define the vector of the 2D-BPFs from Eq. (2).
Step 3: Define the $2D - CWs^{2k}$ from Eq. (8).
Step 4: Make the unknown vector $G_{\mu\times1}(x, y)$ based on the optional nodal points.
Step 5: Compute the vector $F_{\mu\times1}(x, y)$ by considering Eqs. (11) and (13).
Step 6: Compute the $2D - CWs^{2k}$ matrix $\Lambda_{\mu\times\mu}$ from Theorem 2.1.
Step 7: Compute the coefficients matrix $(U_1)_{\mu\times\mu}$ from the Input part and using Eqs. (16) and (17).
Step 8: Compute the matrix $(F_O)_{\mu\times\mu}$ from Eq. (19).
Step 9: Compute the vector $R_{\mu\times1}$ from Eq. (27) and using Steps 4, 7 and 8.
Step 10: Compute the coefficients matrix $(U_2)_{\mu\times\mu}$ from the Input part and using Eqs. (16) and (17).
Step 11: Compute the matrix of $\dot{G}_{\mu\times\mu}$ from Steps 4 and 6, using Point 1.
Step 12: Compute the matrix of $\ddot{G}_{\mu\times\mu}$ from Steps 6 and 11, using Point 1.
Step 13: Compute the matrix of $\overline{Oo}_{\mu\times\mu}$ from Input part, using Lemma 3.1.
Step 14: Compute the matrix of $(V_O)_{\mu\times\mu}$ from Step 6, using Theorem 3.3.
Step 15: Compute the vector $(\grave{J}_O)_{\mu\times1}$ from Steps 6, 10, 12 and 14, using Eq. (25).
Step 16: Compute the vector $(\ddot{J}_O^T)_{\mu\times1}$ from Steps 6 and 15, using Eq. (24).
Step 17: Compute the coefficients matrix $(U_3)_{\mu\times\mu}$ from the Input part and using Eqs. (16) and (17).
Step 18: Compute the matrices of $(\overline{Os}_{a,b})_{\mu\times\mu}$ from Input part, using Lemma 3.2 for $a = 1, 2, ..., \iota_1$, and $b = 1, 2, ..., \iota_2$.
Step 19: Compute the matrix of $(\overline{VS}_{a,b})_{\mu\times\mu}$ from Step 6, using Theorem 3.4 for $a = 1, 2, ..., \iota_1$, and $b = 1, 2, ..., \iota_2$.
Step 20: Compute the vector $(\grave{J}_S)_{\mu\times1}$ from Steps 6, 12, 17 and 19, using Eq. (25).
Step 21: Compute the vector $(\ddot{J}_S^T)_{\mu\times1}$ from Steps 6 and 20, using Eq. (24).
Step 22: Solve the linear system (26).
Step 23: Compute the approximate solution of $\dot{g}(x, y)$ from step 22 and using (21).

6. Numerical Examples

In this section, three different examples are given to the successfully demonstrate of the proposed method in this paper. The numerical results of all three examples show that at almost most nodal points, as the $2D - CWs^{2k}$ orders, i.e., k_1, M_1, k_2, and M_2, increase, the calculated approximate solutions $(\ddot{ApS})$ become closer and closer to the analytical solution $(\ddot{AnS})$ of the desired example. So that it can be admitted that in order to obtain a more accurate solution, the overall $2D - CWs^{2k}$ order, i.e., μ, must be increased. However, increasing μ requires more memory and also more time to perform heavier calculations. Also at almost most examples, the tables and figures confirm that the minimum point error (E_{min}), average error $(\widetilde{E_a})$, and $\overline{L\%95CI}$ in level 81 are smaller than in level 16. Here we note that E_{min} is the absolute error of the method expressed at each of the nodal points, which, based on the results obtained in the tables, is clearly observed to decrease as the approximation level μ increases. In addition, by comparing this method with the $2D - BPFs$ and $2D - HWFs$ methods [9, 10], we find that the current method has better results than other methods in some or most of the points. Table 1, Table 3 and Table 5 display the E_{min} in the optional points (x_i, y_j), the $\widetilde{E_a}$, the $\widetilde{\%95CI}$ for at least 250 runs of our method and the $\overline{L\%95CI}$ along with the levels of $2D - CWs^{2k}$

$$k_1 = k_2 = 1, 2 \ \wedge \ M_1 = M_2 = 2, 4 \ \rightarrow \ \mu = 16, 81,$$

for Examples 6.2, 6.3 and 6.4, respectively with five decimal places. Also for these examples, the comparison of E_{min} and $\widetilde{E_a}$ for the present method in the levels

$$k = k_1 = k_2 = 1, 2 \ \wedge \ M = M_1 = M_2 = 2, 4,$$

with the $2D-HWFs$ method in the levels $J = J_1 = J_2 = 4$, and $2D-BPFs$ method in levels $N = N_1 = N_2 = 2, 4$, are displayed in Table 2, Table 4 and Table 6. On the other hand the reader can see the $3D$-graphs of the $\ddot{AnS}$ and $\ddot{ApS}$ of Examples 6.2, 6.3 and 6.4 with levels $k = 1$, $M = 2$ and $k = 2$, $M = 4$ in Figure 1, Figure 2 and Figure 3, respectively. In conclusion, it can be said that in this calculation process, all the independent variables: k_1, k_2, μ, M_1, M_2, J_1, J_2, N_1 and N_2, which we can choose without restriction, are considered to be degree of freedom items that can be freely changed to achieve greater accuracy and efficiency. We also point out that the two-dimensional noises used in these examples have been considered with five intensities for each dimension. So that we must say that due to the randomness of the functions in the equation, and in two dimensions, naturally, the more the noise intensity is added in each dimension, the higher the process and volume of numerical calculations become, and the longer time must be spent on implementing different numerical methods to solve the desired equation numerically. Basically, this is the same problem that researchers in this field always face in solving stochastic integral equations. Therefore, choosing new techniques and numerical methods to solve such equations has always been a concern of researchers in this field of science.
Before introducing examples of $2D$ stochastic integral equations, we recall that the numerical solution of such equations was first performed in 2015 [27, 28]. From the very beginning, the construction of such examples of $2D$ stochastic integral equations by researchers in this field has been carried out with the help of the following fundamental theorem.

Theorem 6.1 *Suppose $F(t, x)$ is an antiderivative in x of a continuous function $f(t, x)$. Assume that $\frac{\partial F}{\partial t}$ and*

https://doi.org/10.57647/mathsci.2025.1902.09

$\frac{\partial f}{\partial x}$ *are continuous. Then*

$$\int_a^b f(t,B(t))dB(t) = F(t,B(t))\Big|_a^b - \int_a^b \left(\frac{\partial F}{\partial t}(t,B(t)) + \frac{1}{2}\frac{\partial f}{\partial x}(t,B(t))\right)dt.$$

Proof. See [2]. □

Example 6.2 *Consider the 2D.MN.S.VF.LIE*

$$\begin{aligned} g(x,y) &= x+y-\frac{7}{6}-\frac{1}{6}xy(5x^2+9xy+5y^2) \\ &-2xy\sum_{i=1}^{5}\sum_{j=1}^{5}\left(x^2B_i(x)-2\underline{IS}_1(i,x)\right) \\ &\times\left(y^2B_j(y)-2\underline{IS}_1(j,y)\right) \\ &+\int_0^1\int_0^1 (x+y+s+t)g(s,t)dsdt \\ &+\int_0^y\int_0^x (x+y+s+t)g(s,t)dsdt \\ &+\sum_{i=1}^{5}\sum_{j=1}^{5}\int_0^y\int_0^x xystg(s,t)dB_i(S)dB_j(t), \end{aligned}$$

where

$$\underline{IS}_1(a,z) = \int_0^z B_a(s)ds,$$

with the $\dddot{A}nS$

$$g(x,y) = x+y.$$

Example 6.3 *Consider the 2D.MN.S.VF.LIE*

$$\begin{aligned} g(x,y) &= xy\sum_{i=1}^{5}\sum_{j=1}^{5}e^{B_i(x)+B_j(y)} \\ &-\sqrt{xy}\sum_{i=1}^{5}\sum_{j=1}^{5}\underline{S}_1(i)\underline{S}_2(j) \\ &-\sqrt{xy}\sum_{i=1}^{5}\sum_{j=1}^{5}\underline{IS}_2(j,y)\underline{IS}_3(i,x) \\ &-Cos(xy)\sum_{i=1}^{5}\sum_{j=1}^{5}\left(xe^{B_i(x)}-\underline{IS}_4(i,x)\right) \\ &\times\left(ye^{B_j(y)}-\underline{IS}_4(j,y)\right) \\ &+\int_0^1\int_0^1 t\sqrt{xy}Sin(s)g(s,t)dsdt \\ &+\int_0^y\int_0^x t\sqrt{xy}Sin(s)g(s,t)dsdt \\ &+\sum_{i=1}^{5}\sum_{j=1}^{5}\int_0^y\int_0^x stCos(xy)g(s,t)dB_i(s)dB_j(t), \end{aligned}$$

with definitions

$$\underline{S}_1(a) = \int_0^1 sSin(s)e^{B_a(s)}ds,$$

$$\underline{S}_2(a) = \int_0^1 s^2e^{B_a(s)}ds,$$

$$\underline{IS}_2(a,z) = \int_0^z s^2e^{B_a(s)}ds,$$

$$\underline{IS}_3(a,z) = \int_0^z sSin(s)e^{B_a(s)}ds,$$

and

$$\underline{IS}_4(a,z) = \int_0^z e^{B_a(s)}(1+\frac{s}{2})ds,$$

also with the $\dddot{A}nS$

$$g(x,y) = xy\sum_{i=1}^{5}\sum_{j=1}^{5}e^{B_i(x)+B_j(y)}.$$

Example 6.4 *Consider the 2D.MN.S.VF.LIE*

$$\begin{aligned} g(x,y) &= xy\sum_{i=1}^{5}\sum_{j=1}^{5}B_i(x)B_j(y) \\ &-\sin(x+y)\sum_{i=1}^{5}\sum_{j=1}^{5}\underline{S}_3(i)\underline{S}_4(j) \\ &-\frac{1}{\sqrt{x^2+y^2+1}}\sum_{i=1}^{5}\sum_{j=1}^{5}\underline{IS}_5(i,x)\underline{IS}_5(j,y) \\ &-xTan(y)\sum_{i=1}^{5}\sum_{j=1}^{5}\left(\frac{\sqrt[3]{y^4}B_j^2(y)}{2}-\frac{2}{3}\underline{IS}_6(j,y)-\frac{3\sqrt[3]{y^7}}{14}\right) \\ &\times\left(\frac{\sqrt[3]{x^4}B_i^2(x)}{2}-\frac{2}{3}\underline{IS}_6(i,x)-\frac{3\sqrt[3]{x^7}}{14}\right) \\ &+\int_0^1\int_0^1 s^2tSin(x+y)g(s,t)dsdt \\ &+\int_0^y\int_0^x \frac{st}{\sqrt{x^2+y^2+1}}g(s,t)dsdt \\ &+\sum_{i=1}^{5}\sum_{j=1}^{5}\int_0^y\int_0^x xTan(y)\sqrt[3]{st}g(s,t)dB_i(s)dB_j(t), \end{aligned}$$

with definitions

$$\underline{S}_3(a) = \int_0^1 s^3B_a(s)ds,$$

$$\underline{S}_4(a) = \int_0^1 s^2B_a(s)ds,$$

and

$$\underline{IS}_5(a,z) = \int_0^z s^2B_a(s)ds,$$

$$\underline{IS}_6(a,z) = \int_0^z B_a^2(s)\sqrt{s}ds,$$

also with the $\dddot{A}nS$

$$g(x,y) = xy\sum_{i=1}^{5}\sum_{j=1}^{5}B_i(x)B_j(y).$$

Table 1. Numerical results for Example 6.2

μ	(x_i, y_j)	E_{min}	$\widetilde{E_a}$	$\widetilde{\%95CI}$	$\overline{L\%95CI}$
16	$(0, 0.7)$	0.08721	0.40750	$(0.25718, 0.25782)$	0.00064
	$(0.2, 0.7)$	0.01906	0.39591	$(0.53268, 0.53279)$	0.00011
	$(0.7, 0.2)$	0.00525	0.51060	$(0.51024, 0.51018)$	0.00006
	$(0.2, 0.2)$	0.00006	0.06279	$(0.55780, 0.55782)$	0.00002
	$(0.7, 0)$	0.00069	0.10511	$(0.59901, 0.59925)$	0.00024
81	$(0, 0.7)$	0.00503	0.37834	$(0.28488, 0.28897)$	0.00409
	$(0.2, 0.7)$	0.00000	0.07275	$(0.40751, 0.40758)$	0.00001
	$(0.7, 0.2)$	0.00008	0.13260	$(0.56261, 0.56282)$	0.00021
	$(0.2, 0.2)$	0.00000	0.26601	$(0.51540, 0.51541)$	0.00001
	$(0.7, 0)$	0.00000	0.07654	$(0.44234, 0.44236)$	0.00002

Table 2. Comparison of the errors of Example 6.2 with other $2D$-methods

$Method$	$Level$	$E_{min}(0.2, 0.2)$	$\widetilde{E_a}(0.2, 0.2)$	$E_m(0.7, 0)$	$\widetilde{E_a}(0.7, 0)$
$HWFs$	$J = 4$	0.00266	0.05591	0.08470	0.24244
$BPFs$	$N = 4$	0.00505	0.06896	0.00177	0.10154
CWs^{2k}	$k = 1$ $M = 2$	0.00006	0.06279	0.00069	0.10511
CWs^{2k}	$k = 2$ $M = 4$	0.00000	0.26601	0.00000	0.07654

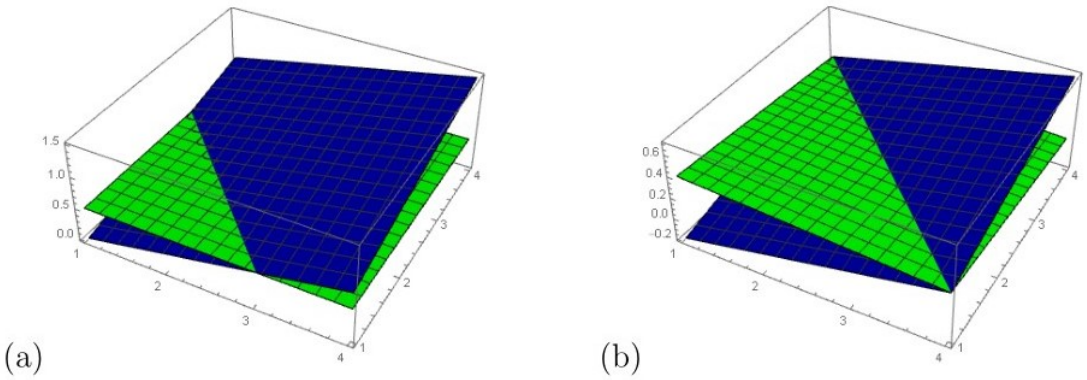

Figure 1. $A\ddot{\overline{n}}S$ and $A\ddot{\overline{p}}S$, Example 6.2, a: $k = 1,\ M = 2$, b: $k = 2,\ M = 4$

Table 3. Numerical results for Example 6.3

μ	(x_i, y_j)	E_{min}	$\widetilde{E_a}$	$\widetilde{\%95CI}$	$\overline{L\%95CI}$
16	$(0, 0.7)$	0.07851	0.21034	$(0.25053, 0.25076)$	0.00023
	$(0.2, 0.7)$	0.06622	0.78053	$(0.36512, 0.36801)$	0.00289
	$(0.7, 0.2)$	0.00588	0.82026	$(0.35418, 0.35442)$	0.00024
	$(0.2, 0.2)$	0.00471	0.33106	$(0.24015, 0.24104)$	0.00089
	$(0.7, 0)$	0.00302	0.25006	$(0.25222, 0.25252)$	0.00030
81	$(0, 0.7)$	0.00001	0.20545	$(-0.16156, 0.00049)$	0.16205
	$(0.2, 0.7)$	0.00008	0.74212	$(-0.18195, 0.00076)$	0.18271
	$(0.7, 0.2)$	0.00595	0.79114	$(-0.35652, -0.35622)$	0.00030
	$(0.2, 0.2)$	0.00005	0.04991	$(-0.22566, -0.22564)$	0.00002
	$(0.7, 0)$	0.00000	0.01133	$(-0.26019, -0.26018)$	0.00001

https://doi.org/10.57647/mathsci.2025.1902.09

Table 4. Comparison of the errors of Example 6.3 with other $2D$-methods

Method	*Level*	$E_{min}(0, 0.7)$	$\widetilde{E_a}(0, 0.7)$	$E_m(0.2, 0.7)$	$\widetilde{E_a}(0.2, 0.7)$
HWFs	$J = 4$	0.01244	0.24051	0.05115	0.79260
BPFs	$N = 4$	0.00560	0.26187	0.04289	0.68303
CWs^{2k}	$k = 1$ $M = 2$	0.07851	0.21034	0.06622	0.78053
CWs^{2k}	$k = 2$ $M = 4$	0.00001	0.10545	0.00008	0.74212

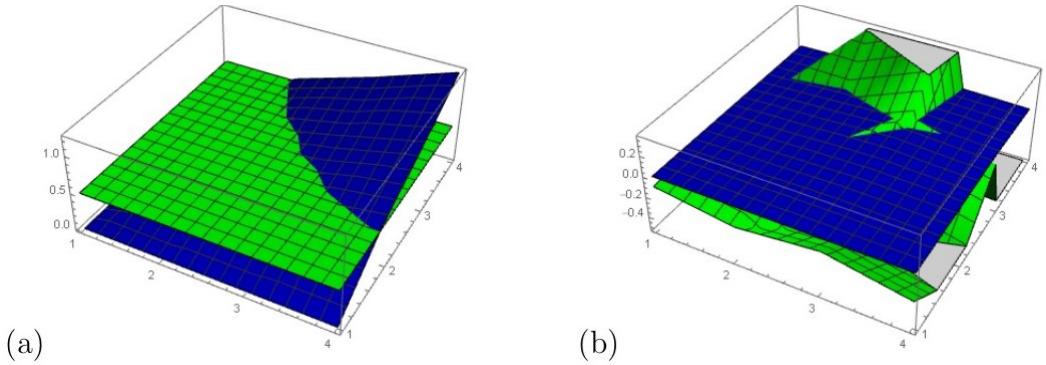

Figure 2. $A\ddot{\overline{n}}S$ and $A\ddot{\overline{p}}S$, Example 6.3, a: $k = 1,\ M = 2$, b: $k = 2,\ M = 4$

Table 5. Numerical results for Example 6.4

μ	(x_i, y_j)	E_{min}	$\widetilde{E_a}$	$\overbrace{\%95CI}$	$\overline{L\%95CI}$
16	$(0, 0.7)$	0.00735	0.50314	$(-0.52271, -0.52266)$	0.000205
	$(0.2, 0.7)$	0.01024	0.53302	$(-0.55626, -0.55617)$	0.00009
	$(0.7, 0.2)$	0.00353	0.36840	$(-0.57581, -0.57579)$	0.00002
	$(0.2, 0.2)$	0.00005	0.13531	$(-0.52610, -0.52608)$	0.000802
	$(0.7, 0)$	0.00915	0.50016	$(-0.53165, -0.53146)$	0.00009
81	$(0, 0.7)$	0.00022	0.29001	$(-0.475..., -0.475...)$	0.00000
	$(0.2, 0.7)$	0.05004	0.18601	$(-0.00066, 0.00012)$	0.00078
	$(0.7, 0.2)$	0.00013	0.02251	$(0.15510, 0.15512)$	0.00002
	$(0.2, 0.2)$	0.00000	0.02442	$(-0.445..., -0.445...)$	0.00000
	$(0.7, 0)$	0.00056	0.10233	$(-0.00123, 0.00017)$	0.00140

Table 6. Comparison of the errors of Example 6.4 with other $2D$-methods

Method	*Level*	$E_{min}(0.2, 0.2)$	$\widetilde{E_a}(0.2, 0.2)$	$E_m(0.7, 0.2)$	$\widetilde{E_a}(0.7, 0.2)$
HWFs	$J = 4$	0.00866	0.34349	0.08010	0.37050
BPFs	$N = 4$	0.00045	0.33501	0.00215	0.42421
CWs^{2k}	$k = 1$ $M = 2$	0.00005	0.13531	0.00353	0.36840
CWs^{2k}	$k = 2$ $M = 4$	0.00000	0.02442	0.00013	0.02251

https://doi.org/10.57647/mathsci.2025.1902.09

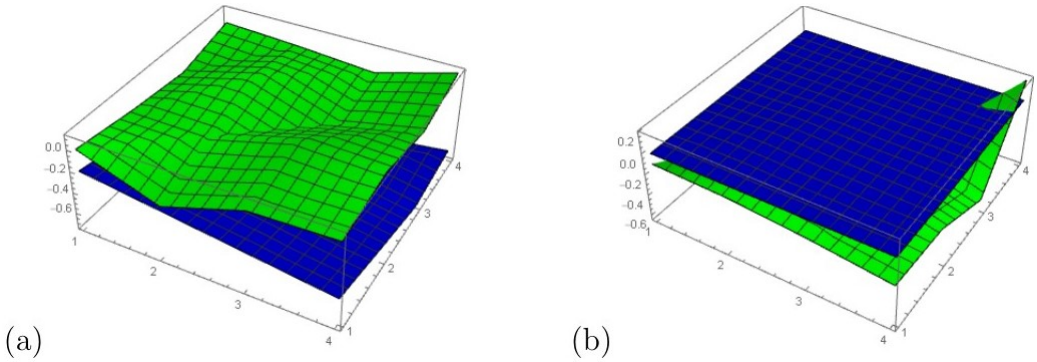

Figure 3. $A\ddot{\bar{n}}S$ and $A\ddot{\bar{p}}S$, Example 6.4, a: $k = 1,\ M = 2$, b: $k = 2,\ M = 4$

Tables analysis:

By looking at Table 1, Table 3 and Table 5, it can be concluded that as the $2D - CWs^{2k}$ level μ increases in our method, the values E_{min}, $\widetilde{E_a}$, $\widetilde{\%95CI}$ and $\overline{L\%95CI}$ decrease in some or most nodal points. In fact, we expect that when we increase the levels k_1, M_1 and k_2, M_2 , we will reach very accurate solutions and close to the $A\ddot{\bar{n}}S$. Also, by checking Table 2, Table 4 and Table 6, it is clearly seen that the errors of the current method are less in some or most points compared to the errors of the $2D - HWFs$ and $2D - BPFs$ methods with the increase of the $2D - CWs^{2k}$ level μ. In general the reduction in E_{min}, with increasing level indicates the efficiency of the proposed method. Also, the reduction in $\widetilde{E_a}$, $\widetilde{\%95CI}$ and $\overline{L\%95CI}$ with increasing level gives us confidence that each of the $A\ddot{\bar{p}}S$s is close to each other, and a further increase in level will make this closeness of the solutions to each other more evident, which results in the convergence of these $A\ddot{\bar{p}}S$s to the $A\ddot{\bar{n}}S$.

Figures analysis:

By carefully observing Figure 1, Figure 2 and Figure 3, it is concluded that in all three of them, in the figures of mode b, where the $2D - CWs^{2k}$ level is 81, the difference between $A\ddot{\bar{n}}S$: $\dot{g}(x, y)$ and $A\ddot{\bar{p}}S$: $g(x, y)$ is less than in mode a, where the this level is 16 in some or most places. Therefore, it is expected that with the increase of the level μ, the $A\ddot{\bar{p}}S$s almost overlap with the $A\ddot{\bar{n}}S$s. This shows the efficiency and accuracy of the proposed method for solving the $2D.MN.S.VF.LIE$ 1.

7. Conclusions

In this study, the $2D - CWs^{2k}$ helped us to solve the $2D.MN.S.VF.LIE$s numerically. In this way, $2D - BPFs$, in combination with these wavelets, facilitated our method for constructing operational matrices. The convergence estimation, the error analysis, and the numerical examples with E_{min}, $\widetilde{E_a}$, $\widetilde{\%95CI}$ and $\overline{L\%95CI}$ all confirmed the accuracy and efficiency of the proposed method. To obtain the $A\ddot{\bar{p}}S$s closer to the $A\ddot{\bar{n}}S$s, it is necessary to increase the order of the wavelet μ, which undoubtedly increases the volume of calculations and their execution time, but even with these small levels, the accuracy of the solutions obtained at some or many nodal points seems reasonable and appropriate. Finally, the combination of other basic functions such as Hat, Laguerre and Hermite with the $2D - BPFs$, can be considered for solving $2D.MN.S.VF.LIE$s in new researchs. .

References

1. Kloeden PE and Platen E. Numerical Solution of Stochastic Differential Equations. Applications of Mathematics. Berlin: Springer-Verlag, 1999
2. Kuo HH. Introduction to Stochastic Integration. New York: Springer Science+Business Media, 2006

3. Klebaner FC. Introduction to Stochastic Calculus with Applications. London: Imperial College Press, 2005
4. Choe GH. Stochastic Analysis for Finance with Simulations. Universitext. Springer, 2016
5. Saha S and Singh S. Numerical solutions of stochastic Volterra-Fredholm integral equations by hybrid Legendre block-pulse functions. Nonlinear Sciences and Numerical Simulation 2018. DOI: 10.1515/ijnsns-2017-0038
6. Mohammadi F. Haar wavelets approach for solving multidimensional stochastic Ito-Volterra integral equations. Applied Mathematics E-Notes 2015; 15:80–96
7. Maleknejad K, Khodabin M, and Rostami M. Numerical solution of stochastic Volterra integral equations by a stochastic operational matrix based on block pulse functions. Mathematical and Computer Modelling 2012; 55:791–800
8. Mohammadi F and Adhami P. Numerical study of stochastic Volterra-Fredholm integral equations by using second kind Chebyshev wavelets. Random Operators and Stochastic Equations 2016; 24:129–41
9. Fallahpour M, Khodabin M, and Maleknejad K. Theoretical error analysis and validation in numerical solution of two-dimensional linear stochastic Volterra-Fredholm integral equation by applying the blockpulse functions. Cogent Mathematics 2017; 4:1296750
10. Fallahpour M, Khodabin M, and Maleknejad K. Theoretical error analysis of solution for two-dimensional stochastic Volterra integral equations by Haar wavelet. International Journal of Applied and Computational Mathematics 2019
11. Fallahpour M, Khodabin M, and Ezzati R. A new computational method based on Bernstein operational matrices for solving two-dimensional linear stochastic Volterra integral equations. Differential Equations and Dynamical Systems 2019
12. Fallahpour M and Khodabin M. Modified Block-Pulse Functions Scheme for Solve of Two-Dimensional Stochastic Integral Equations. Mathematical Sciences and Modelling 2020; 3:38–46
13. Saffarzadeh M, Loghmani GB, and Heydari M. An iterative technique for the numerical solution of nonlinear stochastic Ito-Volterra integral equations. Computational and Applied Mathematics 2018; 333:74–86
14. Alipour S and Mirzaee F. An iterative algorithm for solving two dimensional nonlinear stochastic integral equations: A combined successive approximations method with bilinear spline interpolation. Applied Mathematics and Computation 2020; 371:124947
15. Fallahpour M, Ezzati R, and Hashemizadeh E. A combined efficient method for approximating the solution of two-dimensional integral equations. Discrete Mathematics and Its Applications 2024; 9:269–87
16. Ramadan MA, Raslan KR, and Nassar MA. An approximate solution of systems of high-order linear differential equations with variable coefficients by means of a rational Chebyshev collocation method. Electronic Journal of Mathematical Analysis and Applications 2016; 4:86–98
17. Ramadan MA and Salam MAAE. Spectral collocation method for solving continuous population models by means of exponential Chebyshev approximation. International Journal of Biomathematics 2018; 11:1850109
18. Ramadan MA, Raslan KR, Danaf TSE, and Salam MAAE. A new exponential Chebyshev operational matrix of derivatives for solving high-order ordinary differential equations in unbounded domains. Journal of Modern Methods in Numerical Mathematics 2016. DOI: 10.20454/jmmnm.2016.1068
19. Youssri YH and Atta AG. Optimal third-kind Chebyshev collocation algorithm for solving beam-type micro- and nanoscale boundary value problems. Journal of Mathematical Modeling 2025; 14:841–56
20. Youssri YH, Alnaser LA, and Atta AG. A spectral collocation approach for time-fractional Korteweg–de Vries–Burgers equation via first-kind Chebyshev polynomials. Contemporary Mathematics 2025; 6:1501–19
21. Youssri YH and Atta AG. Adopted Chebyshev collocation algorithm for modeling human corneal shape via the Caputo fractional derivative. Contemporary Mathematics 2025; 6:1223–38
22. Youssri YH and Atta AG. Chebyshev Petrov–Galerkin method for nonlinear time-fractional integro-differential equations with a mildly singular kernel. Journal of Applied Mathematics and Computing 2025; 71:3891–911
23. Safdari H, Aghdam YE, and Gómez-Aguilar JF. Shifted Chebyshev collocation of the fourth kind with convergence analysis for the space–time fractional advection-diffusion equation. Engineering with Computers 2022; 38:1409–20
24. Mesgarani H, Beiranvand A, and Aghdam YE. The impact of the Chebyshev collocation method on solutions of the time-fractional Black–Scholes. Mathematical Sciences 2021; 15:137–43
25. Aghdam YE, Mesgarani H, Moremedi GM, and Khoshkhahtinat M. High-accuracy numerical scheme for solving the space-time fractional advection-diffusion equation with convergence analysis. Alexandria Engineering Journal 2022; 61:217–25

26. Mason JC and Handscomb DC. Chebyshev Polynomials. Boca Raton: CRC Press, 2010

27. Fallahpour M, Maleknejad K, and Khodabin M. Approximation solution of two-dimensional linear stochastic Fredholm integral equation by applying the Haar wavelet. Mathematical Modelling and Computations 2015. Available at arXiv:1505.04855:361–72

28. Fallahpour M, Khodabin M, and Maleknejad K. Approximation solution of two-dimensional linear stochastic Volterra-Fredholm integral equation via two-dimensional Block-pulse functions. Industrial Mathematics 2016; 8:00774

29. Jiang ZH and Schaufelberger W. Block Pulse Functions and Their Applications in Control Systems. Springer-Verlag, 1992

https://doi.org/10.57647/mathsci.2025.1902.09